Analytica Chimica Acta 697 (2011) 90–97

Contents lists available at ScienceDirect

Analytica Chimica Acta

journal homepage: www.elsevier.com/locate/aca

Enhanced electrochemiluminescence from luminol at multi-walled carbon nanotubes decorated with palladium nanoparticles: A novel route for the fabrication of an oxygen sensor and a glucose biosensor

Behzad Haghighi*, Somayyeh Bozorgzadeh

Department of Chemistry, Institute for Advanced Studies in Basic Sciences, P.O. Box 45195-1159, Gava Zang, Zanjan, Iran

ARTICLE INFO

Article history:
Received 9 March 2011
Received in revised form 12 April 2011
Accepted 18 April 2011
Available online 28 April 2011

Keywords:
Electrochemiluminescence
Multi-walled carbon nanotubes
Palladium nanoparticles
Luminol
Oxygen
Glucose

ABSTRACT

Incorporation of palladium nanoparticles on the surface of multi-walled carbon nanotubes and modification of glassy carbon electrode with the prepared nano-hybrid material led to the fabrication of a novel electrode. The modified electrode showed attractive electrocatalytic activity and sensitizing effect on luminol–O_2 and luminol–H_2O_2 electrochemiluminescence (ECL) reactions at neutral media. The sensitized luminol–O_2 and luminol–H_2O_2 reactions were successfully applied for the ECL determination of dissolved O_2 and glucose, respectively. Under the optimal conditions for luminol–O_2 system, the ECL signal intensity of luminol was linear with the concentration of dissolved oxygen in the range between 0.08 and 0.94 mM (r = 0.9996) and for luminol–H_2O_2 system, the ECL signal intensity of luminol was linear with the concentration of glucose in the range between 0.1 and 1000 μM (r = 0.9998). The limits of detection (S/N = 3) for dissolved oxygen and glucose were 0.02 mM and 54 nM, respectively. The relative standard deviations (RSD) for repetitive measurements of 0.50 mM oxygen (n = 10) and 10 μM glucose (n = 30) were 3.5% and 0.3%, respectively. Also, under the optimal conditions for luminol–H_2O_2 system, the ECL signal intensity of luminol was linear with the concentration of H_2O_2 in the range between 1 nM and 0.45 mM (r = 0.9997). The limit of detection (S/N = 3) for H_2O_2 detection was 0.5 nM and the relative standard deviation for repetitive measurements of 10 μM H_2O_2 (n = 10) was 0.8%.

1. Introduction

Successful and extensive applications of ECL for the determination of various species reveal that ECL is an important and valuable detection method in the field of analytical chemistry [1,2]. Luminol is an inexpensive classic organic reagent which can be used for chemiluminescence (CL) and ECL reactions [3,4]. Different mechanistic pathways have been proposed for the ECL reaction of luminol, which partly depend on the applied potential, electrode materials and the electrode surface status [1,5–8]. Luminol ECL reaction takes place in the presence of dissolved oxygen and also hydrogen peroxide but the ECL signal intensity for the later case is higher than the former case. Luminol generates strong CL and ECL signals in alkaline media but, its ECL signals in neutral media are very weak [7]. Recently, several efforts have been devoted to sensitize and apply luminol ECL reaction for the determination of biologically important compounds in their physiological conditions [9–16].

The application of special potential window (range) or constant potential for the generation of reactive oxygen species (ROSs) is one of the ways for the sensitization of luminol ECL reaction [12]. ROSs, include singlet oxygen ($^1O_2$), superoxide hydrogen ($HO_2^{\bullet}$), superoxide radical ($O_2^{\bullet -}$), hydroxyl radical ($OH^{\bullet}$), inorganic or organic peroxides and so on, are generally highly reactive species due to the presence of unpaired valence shell electron. Superoxide and hydroxyl radicals can be generated from the reduction of oxygen during the scan of potential in negative direction and also from the oxidation and reduction of hydrogen peroxide during the scan of potential in positive and negative directions, respectively. These electrogenerated reactive species at the electrode surface can oxidize luminol radical anions, the product of the oxidation of luminol anion at the electrode surface, and consequently produce the excited state 3-aminophthalate anions which emit light [12].

Application of electrodes modified with nano-materials in ECL is another way to sensitize and enhance ECL signals [17,18]. The catalytic and sensitizing effect of metal nanoparticles (NPs) such as Pt-NPs [19], Au-NPs [20–22] and Ag-NPs [23–25] on CL and ECL reactions have been demonstrated for luminol–O_2 and luminol–H_2O_2 systems in alkaline and neutral media. In addition, nano-structure materials such as TiO_2 nanoparticles [26], multi-walled carbon nanotubes (MWCNTs) [11,14,27] and Au-NPs [13] have been also used to enhance ECL signal of luminol–H_2O_2 system in neutral media. The sensitized luminol ECL reactions have

* Corresponding author. Tel.: +98 241 4153 126; fax: +98 2414153 232.
E-mail address: haghighi@iasbs.ac.ir (B. Haghighi).

0003-2670/$ – see front matter © 2011 Elsevier B.V. All rights reserved.
doi:10.1016/j.aca.2011.04.032

been applied for the detection of superoxide dismutase (SOD) based on the quenching effect of SOD on luminol–O_2 ECL system by scavenging reactive oxygen species, for the detection of horseradish peroxidase (HRP) based on its enhancing effect on luminol–O_2 ECL reaction [12], and for the indirect determination of glucose [11,13,14,27] and choline [26] which react with their related enzymes and produce hydrogen peroxide. The sensitized ECL reactions make a possibility for sensitive, simple and inexpensive measurement of dissolved O_2 in the environmental, biomedical and luminol target immunological reactions [12,28–30]. Recently, a novel and robust oxygen gas sensor has been presented by Zhang et al. [31] based on electrochemiluminescence of $Ru(bpy)_3^{3+/+}$ ion annihilation in an ionic liquid medium.

Carbon nanotubes (CNTs) [32] and metal nanoparticles (NPs) are extremely attractive materials because of their unique physical, electrical and catalytic properties [33] with various applications in many research areas. Also, the attachment of metal NPs to CNTs which is often referred as a "decoration" process [34], has led to the creation of a new class of hybrid material with the integrated properties of two components [35]. Palladium NPs (Pd-NPs) are of great interest due to their high electrocatalytic activity for the detection of important analytes with a sluggish redox process such as H_2O_2, nicotinamide adenine dinucleotide (NADH) [36] and hydrazine [37]. Pd-NPs are widely used for O_2 reduction in fuel cells [38]. Also, Pd-NPs can generate hydroxyl radicals during the concomitant reduction of palladium oxide and hydrogen peroxide either added to the solution or produced in situ by oxygen reduction at palladium oxide nanoparticle modified ITO electrodes [39].

To the best of our knowledge, there is only one report in which Pd-NPs supported on functional carbon nanotubes (FCNTs) has been used for the non-enzymatic ECL detection of glucose. In the mentioned study, Pd-NPs–FCNTs catalyze luminol oxidation and glucose dehydrogenization reactions to form glucose radicals which can react with luminol anion radicals to generate the excited state 3-aminophthalate [40].

Herein, Pd-NPs decorated multi-walled carbon nanotubes (nanoPd-MWCNTs) were synthesized by thermal decomposition method and then used to modify glassy carbon electrode (GCE) by casting procedure. Glassy carbon electrode modified with nanoPd-MWCNTs (GCE/nanoPd-MWCNTs) showed excellent electrocatalytic activity and sensitizing effect on luminol–O_2 and luminol–H_2O_2 ECL reactions at neutral media. The proposed modified electrode was successfully applied for the determination of dissolved O_2, luminol, hydrogen peroxide and glucose. The proposed sensor presented high analytical performance in terms of sensitivity, stability, selectivity, linear range and limit of detection.

2. Experimental

2.1. Reagents and chemicals

All chemicals were of analytical reagent grade and used without further purification. Glucose oxidase (GOx, EC 1.1.3.4, type VII from *Aspergillus niger*, 221 U mg^{-1}) and D (+)-glucose (97%) were obtained from Sigma (St. Louis, MO, USA). Nafion perfluorinated ion-exchange (5% solution in 90% light alcohol) was obtained from Fluka (Buchs, Switzerland). Luminol, palladium (II) acetate (47% Pd), sodium hydroxide, dimethylformamide (DMF) were obtained from Merck (Darmstadt, Germany). Multi-walled carbon nanotubes (95% purity, OD = 10–30 nm, ID = 5–10 nm and length = 0.5–500 μm) was purchased from Aldrich (Steinheim, Germany).

A 1.0×10^{-2} M stock solution of luminol (3-aminophthalhydrazide) was prepared by dissolving luminol in a small amount of 0.1 M NaOH. Working solutions of luminol were prepared by diluting the stock solution with phosphate buffer solution (PBS, 0.1 M, pH 7.4). A stock solution of glucose (1 M) was prepared in PBS and stored at 4 °C when it was not in use. The stock solution of glucose was allowed to mutarotate at room temperature for 24 h before use. Double distilled water was used throughout.

Pd-NPs decorated MWCNTs were prepared according to the method reported previously [34] with some modifications [41]. In brief, the treatment of MWCNTs was conducted by refluxing with 70% HNO_3 for 16 h, followed by filtering and thorough washing of the material with deionized water until pH of 7. The acid-treated MWCNTs were dried in a vacuum oven. The pretreated MWCNTs (8 mmol carbon equivalent) were dry mixed with $Pd(CH_3COO)_2$ (0.08 mmol) powder using a mortar and pestle for about 30 min under ambient conditions to prepare Pd-NPs decorated MWCNTs with 1 mol % Pd loading. The solid, homogenous mixture of $Pd(CH_3COO)_2$ and MWCNTs was then transferred to a glass vial and heated in a nitrogen oven to 300 °C over 1 h and held isothermally for 3 h. The product was then collected as the Pd-NPs decorated MWCNTs nano-hybrid (nanoPd-MWCNTs).

Analytical grade O_2 and Ar gases were used for the preparation of solutions saturated with oxygen and argon gases, respectively. Phosphate buffer solution (0.1 M, pH 7.4) saturated with oxygen and argon gases were prepared separately by sparging of O_2 and Ar into the PBS for at least 30 min. The working phosphate buffer solutions (0.1 M, pH 7.4) containing different amounts of oxygen were prepared by mixing different ratios of oxygen and argon saturated phosphate buffer solutions.

2.2. Apparatus and procedure

Cyclic voltammetry (CV) was performed using an Autolab potentiostat–galvanostat model PGSTAT30 (Utrecht, The Netherlands) with a conventional three-electrode set-up in which GCE/nanoPd-MWCNTs or GCE/nanoPd-MWCNTs/GOx/Nafion, an $Ag|AgCl|KCl_{sat}$ electrode and a platinum wire served as the working, reference and auxiliary electrodes, respectively. Electrochemical and ECL measurements were carried out in a 4 mL homemade Teflon ECL cell. The working electrode was mounted in the horizontal position in the ECL cell where its surface was exactly in front of the window of a Hamamatsu photomultiplier module (H7468) (Hamamatsu city, Japan). The photodetector and ECL cell were enclosed in a light-tight black box. The working potential was applied to the working electrode in the standard way using the potentiostat and the output CV and ECL signals were acquired using Autolab NOVA software and a home-written data acquisition program, respectively. A Metrohm 691 pH meter was used for pH adjustments. A digital HQ40d portable dissolved oxygen meter (Hach Company, Loveland, USA) was used to determine the concentration of dissolved oxygen in different working solutions. All measurements were performed at room temperature.

2.3. Fabrication of O_2 sensor and glucose biosensor

The surface of a glassy carbon electrode (GCE, diameter = 3 mm) was polished successively with 0.3 and 0.1 μm alumina paste (Struers, Copenhagen, Denmark) to obtain a mirror finish and then cleaned in water under ultrasonication. One milligram of nanoPd-MWCNTs was dispersed in 1 mL DMF with ultrasonic agitation for an hour to achieve a well-dispersed suspension. 5 μL of the prepared nanoPd-MWCNTs suspension was cast on the surface of GCE and dried in an oven at 50 °C to prepare GCE modified with Pd-NPs decorated MWCNTs (GCE/nanoPd-MWCNTs). The prepared GCE/nanoPd-MWCNTs was directly used as a sensor for O_2 detection. Additionally, 5 μL of PBS containing desired amount of GOx (2.21 U) was pipetted on the surface

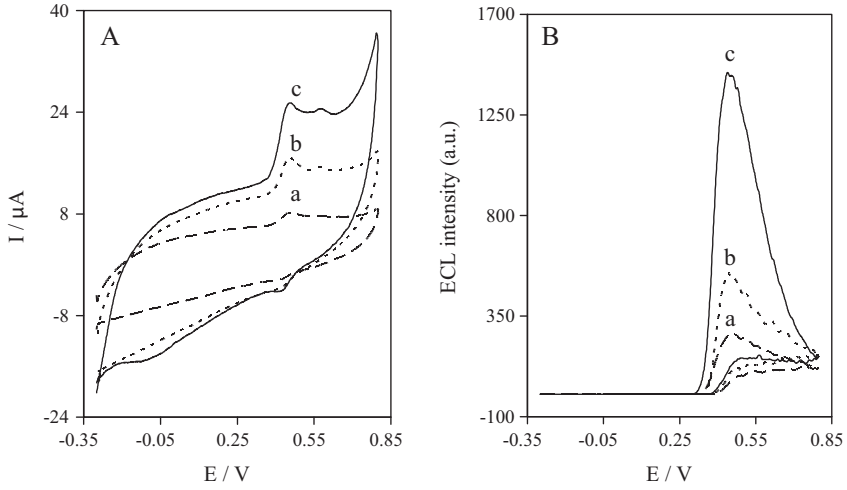

Fig. 1. (A) Cyclic voltammograms and (B) corresponding ECL responses of luminol at a GCE (a), GCE/MWCNTs (b) and GCE/nanoPd-MWCNTs (c). Conditions: luminol, 100 μM; supporting electrolyte, phosphate buffer solution (0.1 M and pH 7.4); potential scan rate, 100 mV s^{-1}.

of GCE/nanoPd-MWCNTs. The GOx modified electrode, GCE/nanoPd-MWCNTs/GOx, was kept at room temperature to dry for about 30 min. Then, 5 μL of Nafion solution (0.5%) was cast on the surface of GCE/nanoPd-MWCNTs/GOx to fabricate glucose biosensor (GCE/nanoPd-MWCNTs/GOx/Nafion). The O_2 sensor and glucose biosensor were stored at room temperature in air and at 4 °C in PBS, respectively, when they were not used. For comparison GCE/MWCNTs, GCE/Nafion and GCE/MWCNTs/Nafion were prepared through similar procedures.

3. Results and discussion

3.1. Characterization of GCE/nanoPd-MWCNTs

SEM image of nanoPd-MWCNTs powder revealed the formation of Pd nanoparticles on the walls of carbon nanotubes with a diameter around 55 ± 5 nm. Cyclic voltammograms of a GCE, GCE/MWCNTs and GCE/nanoPd-MWCNTs were recorded in 0.5 M H_2SO_4 solution at a scan rate of 50 mV s^{-1}. Cyclic voltammogram of the GCE/nanoPd-MWCNTs showed the characteristic current features of Pd reduction (0.38 V) and Pd oxide formation (0.65 V) [41,42]. Also, the appearance of two peaks at −0.092 and 0.036 V during the scan of potential in positive direction and two peaks at −0.09 and −0.28 V during the scan of potential in negative direction was attributed to the adsorption and desorption of hydrogen atoms at and from the electrode surface, respectively [43].

3.2. Electrochemical and ECL behaviors of luminol–O_2 system at GCE/nanoPd-MWCNTs

Fig. 1 shows cyclic voltammograms and corresponding ECL responses (I_{ECL}–E curves) of luminol in PBS at a GCE, GCE/MWCNTs and GCE/nanoPd-MWCNTs in the potential range between −0.3 and 0.8 V versus Ag|AgCl|KCl_{sat} with the scan rate of 100 mV s^{-1}. As shown in Fig. 1A(a), a pair of redox peaks is observed for luminol at the GCE. Modification of GCE with MWCNTs (Fig. 1A(b)) or with nanoPd-MWCNTs (Fig. 1A(c)) caused a significant increase in the redox peaks current intensity of luminol and also in charging current. The ECL responses of luminol at the mentioned different electrodes (Fig. 1B) passed over a maximum at about 0.45 V, which suggested that the luminol oxidation product generates ECL emission. The ECL response intensity of luminol increased 2-fold and 5-fold by modification of the GCE with MWCNTs (Fig. 1B(b)) and with nanoPd-MWCNTs (Fig. 1A(c)), respectively. The increase of charging currents at GCE/MWCNTs and GCE/nanoPd-MWCNTs in comparing with that of GCE was attributed to the increase of electrode surface area because of the presence of MWCNTs and nanoPd-MWCNTs. Also, the enhancement of ECL response intensity, as a result of luminol oxidation, at GCE/MWCNTs in comparing with that of GCE (Fig. 1B(a)) was attributed to the increase of electrode surface area because of the presence of MWCNTs, but the enhancement of ECL response intensity at GCE/nanoPd-MWCNTs in comparing with that of GCE/MWCNTs was attributed to the electrocatalytic activity and sensitizing effect of Pd-NPs on the surface of the MWCNTs, which created more and efficient active sites for the catalytic oxidation of luminol.

Further investigation was performed on ECL behavior of luminol at GCE/nanoPd-MWCNTs by sweeping potential from 0 to −0.3 V followed by −0.3 to 0.8 V (not shown). The observed ECL response intensity was much stronger (about 10-fold) than that of observed at GCE. Moreover, a very strong ECL response (Fig. 2A(c)) was observed for luminol at GCE/nanoPd-MWCNTs by applying reduction potential of −0.3 V for 60 s followed by sweeping potential from −0.3 to 0.8 V. Applying the reduction potential did not show significant enhancement effect on ECL response intensity of luminol at GCE and GCE/MWCNTs. Also, the ECL response intensity at GCE/nanoPd-MWCNTs for luminol was very weak (Fig. 2A(a)) by applying potential only in the range between 0 to 0.8 V. It seemed, sweeping potential in negative direction or applying reduction potential caused the production of species, presumably reactive oxygen species (ROSs), at the electrode surface which could enhance the intensity of luminol ECL response. The presence of cathodic peak at about −0.15 V in Fig. 1A(c) was an evidence for the catalytic activity of nanoPd-MWCNTs toward oxygen reduction.

It was also found that luminol ECL response intensity decreased remarkably by purging of oxygen from the working solution using Ar. But, luminol ECL signal intensity increased significantly by sparging of oxygen into the working solution, suggesting the participation of O_2 in the course of ECL reaction. Also, the results showed that the increase of luminol ECL response intensity in the presence of O_2 at GCE/nanoPd-MWCNTs was higher than those of observed at GCE/MWCNTs and GCE. Electrocatalytic activity of palladium nanoparticles and palladium nanoparticles decorated carbon nanotube modified electrodes toward oxygen reduction [44–47] have been reported, previously. Additionally, it has been reported that the palladium nanoparticles are able to generate hydroxyl radical during the concomitant reduction of palladium oxide and hydrogen

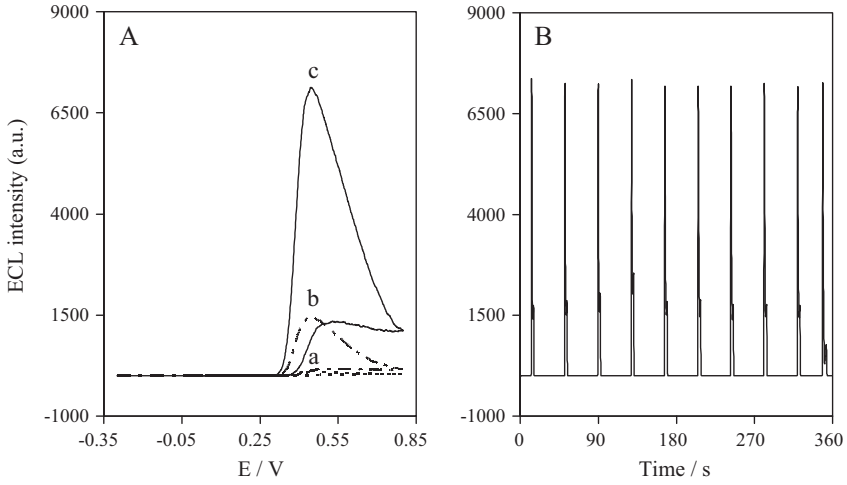

Fig. 2. (A) ECL responses of luminol at GCE/nanoPd-MWCNTs in the potential range between 0 and 0.8 V (a) and in the potential range between −0.3 and 0.8 V without (b) and with (c) applying reduction potential of −0.3 V for 60 s. (B) Reproducibility of ECL responses of luminol at GCE/nanoPd-MWCNTs. Conditions: luminol, 100 μM; supporting electrolyte, phosphate buffer solution (0.1 M and pH 7.4); potential scan rate, 100 mV s^{-1}.

peroxide either added to the solution or produced in situ by oxygen reduction [39]. Accordingly, the great enhancement of luminol ECL response indicates that nanoPd-MWCNTs not only increase the rate of luminol oxidation by their catalytic effect but also increase the amount of reactive oxygen species at the electrode surface by increasing the rate of oxygen reduction.

Therefore, on the basis of the previously reported results and the results obtained in this study for luminol–O_2 ECL system, it is proposed that various reactive oxygen species such as $HO_2^{\bullet}$, $O_2^{\bullet -}$ and $OH^{\bullet}$ as a result of oxygen reduction are produced at the GCE/nanoPd-MWCNTs by applying reduction (negative) potential. During the course of sweeping potential in positive (oxidation) direction luminol is oxidized to the luminol radical anion with the maximum peak current intensity at about 0.45 V. The subsequent chemical reaction of luminol radical anions with reactive oxygen species creates ECL signal, which nanoPd-MWCNTs significantly enhance the ECL signal by increasing the amount of various electrogenerated reactive oxygen species from the reduction of dissolved oxygen at negative potential and also by increasing the amount of luminol oxidation product, luminol radical anions, via accelerating the oxidation rate of luminol. The previous reports on luminol ECL mechanism [1,5–8,12] are in agreement with the proposed mechanistic pathway.

The effect of the loading of nanoPd-MWCNTs at the GCE surface, applied reduction potential, applied reduction time and potential scan rate on luminol ECL signal intensity was investigated to optimize the experimental conditions for the determination of luminol and dissolved oxygen. The results showed at the fixed concentrations of luminol (100 μM) and dissolved oxygen (0.29 mM), the luminol ECL signal intensity increased with increasing the amount of nanoPd-MWCNTs and reached a plateau when 5 μL of nanoPd-MWCNTs (1 mg mL^{-1}) was cast. So, 5 μL of nanoPd-MWCNTs (1 mg mL^{-1}) was selected for the sensor fabrication. Changing the applied reduction potential from 0 to −0.5 V, reduction time from 0 to 120 s and potential scan rate from 10 to 200 mV s^{-1} caused the luminol ECL intensity passed over a maximum at about the reduction potential of −0.3 V, reduction time of 60 s and scan rate of 100 mV s^{-1}.

The analytical applicability of the proposed sensor, GCE/nanoPd-MWCNTs, for ECL determination of luminol and dissolved oxygen was explored at the optimized conditions, i.e. by applying reduction potential of −0.3 V for 60 s followed by sweeping potential from −0.3 to 0.8 V at the scan rate of 100 mV s^{-1}. The ECL signal intensity at the fixed concentration of oxygen (0.29 mM) was linear with the concentration of luminol in the range between 50 nM and 100 μM (r = 0.9997). The sensitive determination of luminol is necessary for some immunological determinations [28,29,48]. Also, the ECL signal intensity of luminol (100 μM) was linear with the concentration of dissolved oxygen in the range between 0.08 and 0.94 mM (r = 0.9996). The limits of detection (signal to noise ratio = 3) for luminol and dissolved oxygen were 8 nM and 0.02 mM, respectively. The relative standard deviations (RSD) for repetitive measurements (n = 10) of 100 μM luminol (Fig. 2B) and 0.50 mM oxygen were 0.7% and 3.5%, respectively. The analytical features of some reported ECL based oxygen sensors using modified electrodes with different modification strategies are summarized in Table 1 and compared with those obtained in this study using GCE/nanoPd-MWCNTs. Fig. 3 presents a typical I_{ECL}–E and its corresponding calibration curve obtained for different concentrations of dissolved oxygen.

3.3. Electrochemical and ECL behaviors of luminol–H_2O_2 system at GCE/nanoPd-MWCNTs/Nafion

Fig. 4 shows cyclic voltammograms and corresponding I_{ECL}–E curves of a PBS containing luminol (100 μM) and H_2O_2 (10 μM) at a GCE/Nafion, GCE/MWCNTs/Nafion and GCE/nanoPd-MWCNTs/Nafion in the potential range between 0 and 0.8 V versus Ag|AgCl|KCl_{sat} with the scan rate of 100 mV s^{-1}. A pair of redox peaks was observed for luminol at about 0.45 V versus Ag|AgCl|KCl_{sat} at GCE/nanoPd-MWCNTs/Nafion (Fig. 4A(c)) and at GCE/MWCNTs/Nafion (Fig. 4A(b)) and no well defined redox peak at GCE/Nafion (Fig. 4A(a)). It can be clearly seen that nanoPd-MWCNTs significantly increase the intensity of luminol oxidation peak cur-

Table 1
Analytical parameters reported for some ECL based O_2 sensors.

Electrode	ECL system	LDR	DL	Refs.
PCE chip/IL	$Ru(bpy)_3^{2+}$	0–40%	0.04%	[31]
GCE/Nafion/$Ru(bpy)_3^{2+}$	$Ru(bpy)_3^{2+}$	0–0.3 mM	nr	[49]
GCE/TiO_2/Nafion	TiO_2	0.3–10 mg/L	0.12 mg/L	[30]
Ti foil/TiO_2 nanotubes	TiO_2	20–80%	nr	[50]
Pt	Luminol	0–16 mg/L	nr	[12]
Au/IL	Luminol	nr	nr	[51]
GCE/Nafion-nano-TiO_2	Luminol	0.05–10 mg/L	0.02 mg/L	[52]
GCE/nanoPd-MWCNTs	Luminol	0.08–0.94 mM	0.02 mM	This work

LDR, linear dynamic range; DL, detection limit; GCE, glassy carbon electrode; IL, ionic liquid; PCE, printed carbon electrode; nr, not reported.

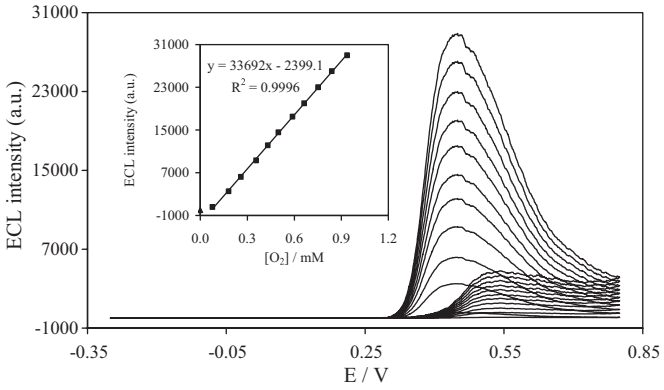

Fig. 3. ECL responses of luminol at GCE/nanoPd-MWCNTs toward different concentrations of oxygen. Inset: calibration plot of ECL responses versus concentration of oxygen. Conditions: luminol, 100 μM; supporting electrolyte, phosphate buffer solution (0.1 M and pH 7.4); reduction potential, −0.3 V for 60 s; potential scan rate, 100 mV s^{-1}.

rent and also the ECL response of luminol–H_2O_2 system. The electrocatalytic property of Pd-NPs on H_2O_2 oxidation reaction has been shown in previous study [36]. It seems luminol ECL reaction can be sensitized by H_2O_2 (by itself) and also by the generated oxygen and superoxide radical anion during the oxidation of H_2O_2 at the electrode surface [12]. Therefore, the observed enhancements in both CV and ECL responses at GCE/nanoPd-MWCNTs/Nafion are attributed to the electrocatalytic activity of nanoPd-MWCNTs on luminol and H_2O_2 oxidation reactions.

The effect of the loading of nanoPd-MWCNTs at the GCE surface and potential scan rate on luminol ECL signal intensity was investigated to optimize the experimental conditions for the determination of hydrogen peroxide. The results showed at the fixed concentrations of luminol (100 μM) and hydrogen peroxide (10 μM), the luminol ECL signal intensity increased with increasing the amount of nanoPd-MWCNTs and reached a plateau when 5 μL of nanoPd-MWCNTs (1 mg mL^{-1}) was cast, the same as that observed for GCE/nanoPd-MWCNTs sensor. So, 5 μL of nanoPd-MWCNTs (1 mg mL^{-1}) was selected for the sensor fabrication. The effect of potential scan rate (υ) on the oxidation peak current intensity of luminol and on its ECL signal intensity in the presence of 10 μM H_2O_2 showed that the oxidation peak current intensity increased linearly with $\upsilon^{1/2}$ in the range between 25 and 200 mV s^{-1}, revealing a diffusion-controlled redox process. Also, the results showed that the ECL signal intensity increased with increasing υ and passed over a maximum at about the scan rate of 100 mV s^{-1}. The ECL responses of the proposed sensor, GCE/nanoPd-MWCNTs/Nafion, in a PBS solution containing 100 μM luminol and different concentrations of H_2O_2 were recorded under optimized conditions by scanning potential between 0 and 0.8 V versus Ag|AgCl|KCl_{sat} at a scan rate of 100 mV s^{-1}. The ECL response was linear with the concentration of H_2O_2 in the range between 1 nM and 0.45 mM with a correlation coefficient of 0.9997. The limit of detection (S/N = 3) for H_2O_2 detection was 0.5 nM. The relative standard deviation for repetitive measurements (n = 10) of 10 μM H_2O_2 was 0.8%.

3.4. Analytical performance of GCE/nanoPd-MWCNTs/GOx/Nafion for glucose detection

Based on the electrocatalytic effect of nanoPd-MWCNTs on luminol–H_2O_2 ECL reaction, GCE/nanoPd-MWCNTs/Nafion was further modified with GOx to fabricate an ECL glucose biosensor. Scheme 1 demonstrates the possible ECL reaction mechanism for the proposed ECL glucose biosensor. GOx catalyzes the oxidation of glucose to produce hydrogen peroxide. Under sweeping potential in positive direction (oxidation), the immobilized nanoPd-MWCNTs on the surface of GCE catalyze the electrochemical oxidation of luminol and the enzymatically produced hydrogen peroxide (not shown). The produced luminol radical anions are further oxidized by the enzymatically produced hydrogen peroxide directly and by electrochemically produced ROSs, as the products of hydrogen peroxide oxidation at the electrode surface (not shown), to give the excited state 3-aminophthalate anions that emit light at about 425 nm.

The effect of GOx and Nafion loadings on the ECL signal intensity of the biosensor, GCE/nanoPd-MWCNTs/GOx/Nafion, was investigated by applying different amounts of GOx and Nafion during the course of biosensor fabrication. Then, their ECL responses were recorded in a PBS containing 100 μM luminol and 10 μM glucose by scanning potential between 0 and 0.8 V versus Ag|AgCl|KCl_{sat} at a scan rate of 100 mV s^{-1}. The results showed that the ECL signal intensity increased with increasing the amount of GOx and then reached a plateau at about 2.21 U GOx. Also, the ECL intensity increased with increasing the concentration of Nafion and reached a maximum at about 0.5% (v/v) Nafion, then the ECL intensity decreased. So, 2.21 U GOx and 5 μL of Nafion solution (0.5%) were used for the fabrication of ECL glucose biosensor. The analytical applicability of the fabricated ECL biosensor was examined for glucose determination using a series of standard glucose solutions,

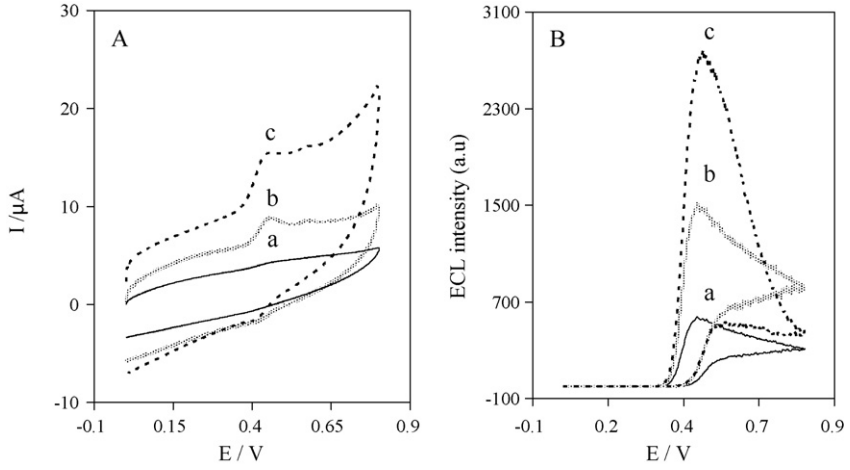

Fig. 4. (A) Cyclic voltammograms and (B) corresponding ECL responses of luminol at a GCE/Nafion (a), GCE/MWCNTs/Nafion (b) and GCE/nanoPd-MWCNTs/Nafion (c). Conditions: luminol, 100 μM; H_2O_2, 10 μM; supporting electrolyte, phosphate buffer solution (0.1 M and pH 7.4); potential scan rate, 100 mV s^{-1}.

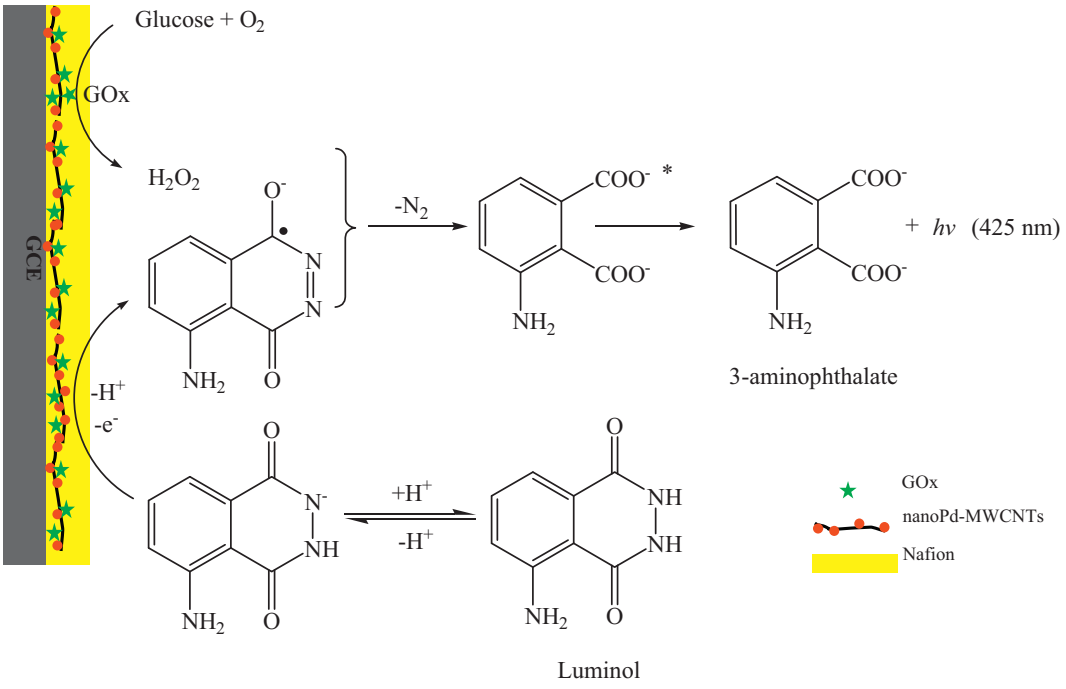

Scheme 1. The possible ECL reaction mechanism for the proposed ECL glucose biosensor.

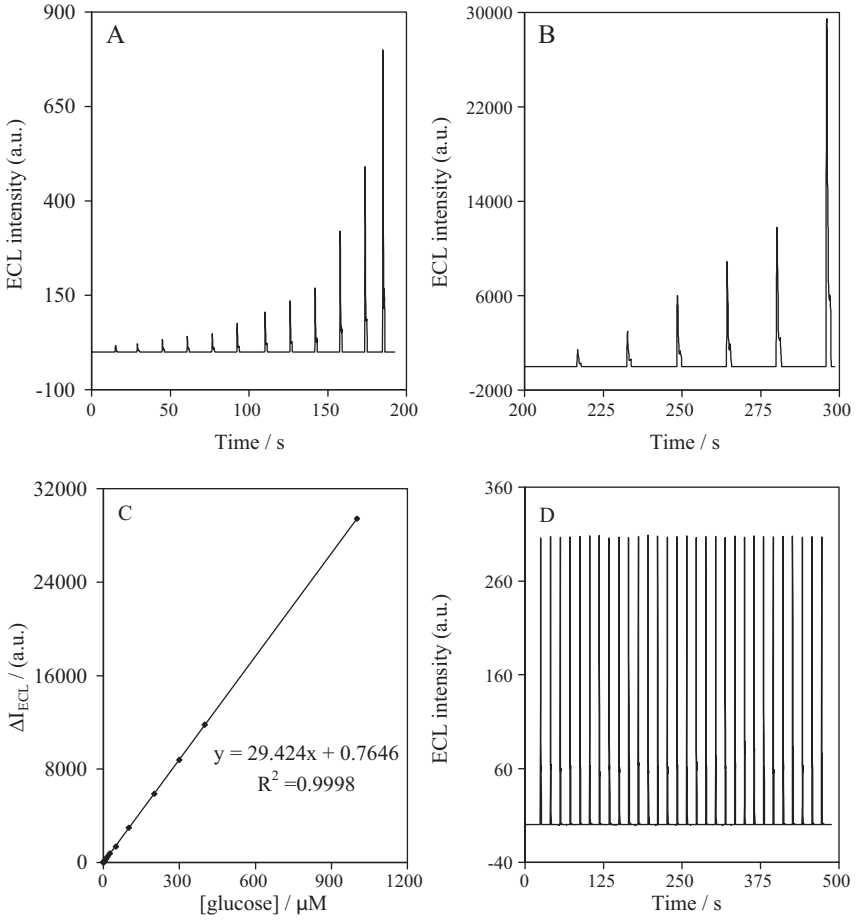

Fig. 5. Typical ECL responses of luminol (100 μM) at GCE/nanoPd-MWCNTs/GOx/Nafion in the presence of glucose in the concentration ranges from (A) 0.1 to 25 μM and (B) 50 to 1000 μM. (C) Calibration plot of ECL responses versus concentration of glucose. (D) Reproducibility of ECL responses in the presence of 10 μM glucose. Conditions: supporting electrolyte, phosphate buffer solution (0.1 M and pH 7.4); scan rate, 100 mV s^{-1}.

Table 2
Analytical parameters reported for some luminol based ECL glucose biosensors.

Modified electrode	LDR (μM)	DL (μM)	pH	Refs.
CNTPE	1–2000	0.5	7	[14]
GCE/CNTs/Nafion	5–80	2	7.4	[27]
Au/sol–gel/AuNPs	1–5000	0.2	7.5	[13]
GCE/MWCNTs/polyNiTSPc/Nafion	1–100	0.08	7.4	[11]
SCPE/Fe_3O_4	10–10,000	1	8	[53]
GCE/Graphene/Nafion	2–100	1	7.4	[54]
GE/PLANC	0.1–50	0.03	9	[55]
GCE/collagen membrane	0.6–3000[a]	0.06[a]	8.5	[56]
GCE/polyamide membrane	1.5–300[a]	1.5[a]	8.5	[56]
GCE/sol gel matrix	50–10,000	26	9	[57]
CCE	10–10,000	8.16	8.5	[58]
SP graphite electrode microarrays	3–3000	3	nr	[59]
GCF-biochip	20–2000	20	8.5	[60]
GCE/PDDA-CS	0.0005–40	0.0001	7.5	[26]
GCE/AuNPs-MWCNTs/CS	1–1000 0.5–110	0.5 0.06	7.4 8.5	[61]
GCE/nanoPd-MWCNTs/Nafion	0.1–1000	0.054	7.4	This work

LDR, linear dynamic range; DL, detection limit; AuNPs, gold nanoparticles; CCE, ceramic carbon composite electrode; CNTPE, carbon nanotubes paste electrode; CNTs, carbon nanotubes; CS, chitosan; GCE, glassy carbon electrode; GCF, glassy carbon foil; GE, graphite electrode; MWCNTs, multi-walled carbon nanotubes; PDDA, poly(diallyldimethylammonium chloride); PLANC, Poly(luminol-aniline) nanowires composite; poly NiTSPc, poly(nickel(II)tetrasulfophthalocyanine); SCPE, solid paraffin carbon paste electrode; SP, screen printed; nr, not reported.

[a] nmol.

under optimized conditions stated above. The ECL calibration curve for glucose detection was linear between the concentration of 0.1 and 1000 μM glucose with the correlation coefficient of 0.9998. The limit of detection (S/N = 3) was 54 nM glucose. The relative standard deviation for repetitive measurements (n = 30) of 10 μM glucose was 0.3%. The fabrication reproducibility for five electrodes prepared and used on different days was 8.6%. The analytical features of some reported luminol based ECL glucose biosensors using modified electrodes with different modification strategies are summarized in Table 2 and compared with those obtained in this study using GCE/nanoPd-MWCNTs/GOx/Nafion. The limit of detection and linear dynamic range of the proposed ECL glucose biosensor were better than those reported for the fabricated ECL glucose biosensors using nano-structured materials such as GCE modified with CNTs–GOx–Nafion composite [27], GCE modified with MWCNTs/poly(nickel(II)tetrasulfophthalocyanine)/GOx/Nafion [11], carbon nanotube paste/glucose oxidase (CNTP/GOx) electrode [14] and GOx/AuNPs/sol-gels/Au electrode [13]. Fig. 5 shows typical ECL traces recorded for glucose using proposed ECL glucose biosensor. The operational stability of the proposed ECL glucose biosensor was also examined by monitoring of its ECL response toward 10 μM glucose every day over a week. It was found that the response of the ECL biosensor gradually decreased to almost 76% of its initial value after one week. The biosensor was kept at 4 °C in 0.1 M PBS between experiments.

3.5. Interference study

The effects of the presence of potential interfering biological compounds such as glycine, alanine, fructose, maltose, sucrose, galactose, uric acid, ascorbic acid and dopamine on the ECL signal intensity of the proposed ECL glucose biosensor were investigated. A series of solutions containing 100 μM glucose plus potential interfering compounds were prepared. The ECL signals of the prepared test solutions were recorded and compared with that obtained for the standard glucose solution (100 μM). A 5% error criterion was adopted. There was no interference from glycine, alanine, fructose, maltose, sucrose and galactose at the concentration about 0.01 M (100-fold). The maximum permissible concentrations for ascorbic acid, uric acid and dopamine were 50 μM, 50 μM and 5 μM, respectively. Ascorbic acid and uric acid at the concentrations about 100 μM decreased the ECL signal intensity of 100 μM glucose for 15% and 21%, respectively. Dopamine at the concentration about 10 μM decreased the ECL signal intensity for 25%. The results are summarized in Table 3.

Table 3
Effect of potential interfering compounds on the ECL signal intensity of 100 μM glucose.

Interfering compounds	Maximum permission concentration[a] (μM)	Relative response[b] (%)
Sucrose	10,000	120 (20,000)
Maltose	10,000	140 (20,000)
Fructose	10,000	110 (20,000)
Galactose	10,000	130 (20,000)
Glycine	10,000	80 (20,000)
Alanine	10,000	85 (20,000)
Ascorbic acid	50	85 (100)
Uric acid	50	79 (100)
Dopamine	5	75 (10)

[a] Concentration of interfering compound which was caused less than 5% error on glucose determination.

[b] The ratio of ECL signal intensity of a glucose solution containing intolerable concentration of interfering compound to the ECL signal intensity of a standard glucose solution. Numbers in the parentheses indicate the intolerable concentrations of interfering compounds in μM.

3.6. Application of biosensor for determination of glucose in normal human serum sample

The proposed ECL biosensor was applied for the determination of glucose in normal human serum to examine its applicability for real sample analysis. 10 μL of the human serum was mixed with 3 mL PBS containing 100 μM luminol and certain amount of glucose and then analyzed using the proposed ECL biosensor. The concentration of glucose in normal human serum determined using the proposed biosensor was 4.82 mM. The recovery of the analysis was about 103%, considering the value determined by local hospital (4.67 mM). Also, to examine the reliability of the proposed biosensor certain amounts of standard glucose solution (10, 30, 50, 150 and 250 μM) was added to the normal human serum solution (3 mL PBS containing 10 μL of the human serum and 100 μM luminol) and analyzed using the proposed biosensor. Recovery of each measurement was calculated by comparing the results obtained before and after adding of standard glucose solution. Recoveries for the spiked samples were between 97% and 103%.

4. Conclusions

Multi-walled carbon nanotubes decorated with palladium nanoparticles was presented as a novel nano-hybrid material with attractive enhancement and sensitizing effect on luminol–O_2 and luminol–H_2O_2 ECL systems at neutral media. The observed enhancement effect on luminol ECL signal intensity was attributed the electrocatalytic activity of nanoPd-MWCNTs toward O_2 reduction, H_2O_2 oxidation and also luminol oxidation reactions. Two ECL systems based on the electrocatalytic activity of nanoPd-MWCNTs on luminol–O_2 and luminol–H_2O_2 ECL reactions were introduced and successfully used for ECL determination of dissolved O_2, luminol, hydrogen peroxide and glucose. The proposed ECL systems presented a number of attractive features such as wide linear range, low limit of detection, excellent reproducibility and satis-

factory stability and selectivity. Application of nanoPd-MWCNTs nano-hybrid for modification of the electrode surface may create a new opportunity for the development of new sensitized ECL sensors and biosensors which can be used in a variety of fields such as clinical diagnostics, immunological analysis and environmental monitoring due to their simplicity and high efficiency.

Acknowledgement

The authors acknowledge the Institute for Advanced Studies in Basic Science (IASBS, Grant Number G2011IASBS119), for financial support.

References

[1] H. Cui, G.-Z. Zou, X.-Q. Lin, Anal. Chem. 75 (2003) 324–331.
[2] L. Hu, G. Xu, Chem. Soc. Rev. 39 (2010) 3275–3304.
[3] M.M. Richter, Chem. Rev. 104 (2004) 3003–3036.
[4] C. Marquette, L. Blum, Anal. Bioanal. Chem. 385 (2006) 546–554.
[5] S. Sakura, Anal. Chim. Acta 262 (1992) 49–57.
[6] H. Cui, Y. Xu, Z.-F. Zhang, Anal. Chem. 76 (2004) 4002–4010.
[7] H.-X. Yu, H. Cui, J. Electroanal. Chem. 580 (2005) 1–8.
[8] W. Wang, H. Cui, Z.-X. Deng, Y.-P. Dong, J.-Z. Guo, J. Electroanal. Chem. 612 (2008) 277–287.
[9] W. Miao, Chem. Rev. 108 (2008) 2506–2553.
[10] X.-M. Chen, B.-Y. Su, X.-H. Song, Q.-A. Chen, X. Chen, X.-R. Wang, TrAC, Trends Anal. Chem. 30 (2011) 665–676.
[11] B. Qiu, Z. Lin, J. Wang, Z. Chen, J. Chen, G. Chen, Talanta 78 (2009) 76–80.
[12] H.H. Chu, W.Y. Guo, J.W. Di, Y. Wu, Y.F. Tu, Electroanalysis 21 (2009) 1630–1635.
[13] X.Q. Liu, W.X. Niu, H.J. Li, S. Han, L.Z. Hu, G.B. Xu, Electrochem. Commun. 10 (2008) 1250–1253.
[14] J.H. Chen, Z.Y. Lin, G.N. Chen, Anal. Bioanal. Chem. 388 (2007) 399–407.
[15] L. Zhang, D. Li, W. Meng, Q. Huang, Y. Su, L. Wang, S. Song, C. Fan, Biosens. Bioelectron. 25 (2009) 368–372.
[16] S. Xu, Y. Liu, T. Wang, J. Li, Anal. Chem. 82 (2010) 9566–9572.
[17] H. Qi, Y. Peng, Q. Gao, C. Zhang, Sensors 9 (2009) 674–695.
[18] P. Bertoncello, R.J. Forster, Biosens. Bioelectron. 24 (2009) 3191–3200.
[19] X.M. Chen, Z.J. Lin, Z.M. Cai, X. Chen, M. Oyama, X.R. Wang, J. Nanosci. Nanotechnol. 9 (2009) 2413–2420.
[20] Z.F. Zhang, H. Cui, C.Z. Lai, L.J. Liu, Anal. Chem. 77 (2005) 3324–3329.
[21] Y.P. Dong, H. Cui, C.-M. Wang, J. Phys. Chem. B 110 (2006) 18408–18414.
[22] Y.P. Dong, H. Cui, Y. Xu, Langmuir 23 (2007) 523–529.
[23] C.M. Wang, H. Cui, Luminescence 22 (2007) 35–45.
[24] J.Z. Guo, H. Cui, W. Zhou, W. Wang, J. Photochem. Photobiol., A 193 (2008) 89–96.
[25] B. Haghighi, S. Bozorgzadeh, Microchem. J. 95 (2010) 192–197.
[26] H. Dai, Y.W. Chi, X.P. Wu, Y.M. Wang, M.D. Wei, G.N. Chen, Biosens. Bioelectron. 25 (2009) 1414–1419.
[27] Z.Y. Lin, J.H. Chen, G.N. Chen, Electrochim. Acta 53 (2008) 2396–2401.
[28] D.Y. Tian, C.F. Duan, W. Wang, H. Cui, Biosens. Bioelectron. 25 (2010) 2290–2295.
[29] D. Tian, C. Duan, W. Wang, N. Li, H. Zhang, H. Cui, Y. Lu, Talanta 78 (2009) 399–404.
[30] Z. Lin, Y. Liu, G. Chen, Electrochem. Commun. 10 (2008) 1629–1632.
[31] L.H. Zhang, F. Tsow, E. Forzani, N.J. Tao, Chem. Commun. 46 (2010) 3333–3335.
[32] S. Iijima, Nature 354 (1991) 56–58.
[33] G.G. Wildgoose, C.E. Banks, R.G. Compton, Small 2 (2006) 182–193.
[34] Y. Lin, K.A. Watson, M.J. Fallbach, S. Ghose, J.G. Smith, D.M. Delozier, W. Cao, R.E. Crooks, J.W. Connell, ACS Nano 3 (2009) 871–884.
[35] V. Georgakilas, D. Gournis, V. Tzitzios, L. Pasquato, D.M. Guldi, M. Prato, J. Mater. Chem. 17 (2007) 2679–2694.
[36] J.S. Huang, D.W. Wang, H.Q. Hou, T.Y. You, Adv. Funct. Mater. 18 (2008) 441–448.
[37] Y. Shen, Q. Xu, H. Gao, N.N. Zhu, Electrochem. Commun. 11 (2009) 1329–1332.
[38] A.A. Gewirth, M.S. Thorum, Inorg. Chem. 49 (2010) 3557–3566.
[39] J. Liu, G. Lagger, P. Tacchini, H.H. Girault, J. Electroanal. Chem. 619–620 (2008) 131–136.
[40] X.M. Chen, Z.M. Cai, Z.J. Lin, T.T. Jia, H.Z. Liu, Y.Q. Jiang, X. Chen, Biosens. Bioelectron. 24 (2009) 3475–3480.
[41] B. Haghighi, H. Hamidi, S. Bozorgzadeh, Anal. Bioanal. Chem. 398 (2010) 1411–1416.
[42] G. Chen, Z.Y. Wang, T. Yang, D.D. Huang, D.G. Xia, J. Phys. Chem. B 110 (2006) 4863–4868.
[43] S. Guerin, G.S. Attard, Electrochem. Commun. 3 (2001) 544–548.
[44] C.C. Yang, A.S. Kumar, J.M. Zen, Electroanalysis 18 (2006) 64–69.
[45] M.H. Shao, T. Huang, P. Liu, J. Zhang, K. Sasaki, M.B. Vukmirovic, R.R. Adzic, Langmuir 22 (2006) 10409–10415.
[46] A.H. Creus, Y. Gimeno, P. Diaz, L. Vazquez, S. Gonzalez, R.C. Salvarezza, A.J. Arvia, J. Phys. Chem. B 108 (2004) 10785–10795.
[47] Y.H. Lin, X.L. Cui, X.R. Ye, Electrochem. Commun. 7 (2005) 267–274.
[48] T. Jiao, B.D. Leca-Bouvier, P. Boullanger, L.J. Blum, A.P. Girard-Egrot, Colloids Surf., A 321 (2008) 143–146.
[49] L. Zheng, Y. Chi, Q. Shu, Y. Dong, L. Zhang, G. Chen, J. Phys. Chem. C 113 (2009) 20316–20321.
[50] L. Chen, L. Lu, Y. Mo, Z. Xu, S. Xie, H. Yuan, D. Xiao, M.M.F. Choi, Talanta (2011), doi:10.1016/j.talanta.2011.03.011.
[51] J. Rong, Y. Chi, Y. Zhang, L. Chen, G. Chen, Electrochem. Commun. 12 (2010) 270–273.
[52] R. Ye, L. Huang, B. Qiu, Z. Song, Z. Lin, G. Chen, Luminescence (2011), doi:10.1002/bio.1265.
[53] Z.G. Xiong, J.P. Li, L. Tang, Z.Q. Cheng, Chinese J. Anal. Chem. 38 (2010) 800–804.
[54] X.P. Chen, H.Z. Ye, W.Z. Wang, B. Qui, Z.Y. Lin, G.N. Chen, Electroanalysis 22 (2010) 2347–2352.
[55] G.X. Li, J.L. Lian, X.W. Zheng, J. Cao, Biosens. Bioelectron. 26 (2010) 643–648.
[56] C.A. Marquette, L.J. Blum, Anal. Chim. Acta 381 (1999) 1–10.
[57] L. Zhu, Y.X. Li, G.Y. Zhu, Sensor. Actuat. B-Chem. 86 (2002) 209–214.
[58] L. Zhu, Y. Li, F. Tian, B. Xu, G. Zhu, Sensor. Actuat. B-Chem. 84 (2002) 265–270.
[59] B.P. Corgier, C.A. Marquette, L.J. Blum, Anal. Chim. Acta 538 (2005) 1–7.
[60] C.A. Marquette, A. Degiuli, L.J. Blum, Biosens. Bioelectron. 19 (2003) 433–439.
[61] B. Haghighi, S. Bozorgzadeh, L. Gorton, Sensor. Actuat B-Chem. (2011), doi:10.1016/j.snb.2011.01.010.